PRINT ISSN 3009-6049
ONLINE ISSN 3009-6022

Soil-Structure Interaction Assessment for Seismic Performance of High-Rise RC Building on Piled-Raft Foundation

Waleed Dawoud[1], Mostafa Nazim[*1], Osama El-Mahdy[1], Maher Adam[1]

[1] Department of Civil Engineering, Faculty of Engineering at Shoubra, Benha University, Cairo, Egypt
[*] Corresponding Author.

E-mail: walid.dawoud@feng.bu.edu.eg, mostafa.saied@feng.bu.edu.eg, osama.alhenawy@feng.bu.edu.eg, maher.adam@feng.bu.edu.eg

Abstract: **.** Seismic design for high-rise structures requires determining the expected base shear, inter-story drift of each story level, and structural elements internal forces. Dealing with the base of structures as a fixed support has many disadvantages and not always conservative. Soil-structure interaction (SSI) represents more realistic and accurate simulation to seismic response of structures as it evaluates the collective response of the structure, the foundation, and the subsurface lithology to a specified ground motion. Present study focuses on the direct approach of soil-structure interaction analysis of a three-dimensional high-rise reinforced concrete building over piled-raft foundation. Fully nonlinear numerical analysis using finite element method was utilized and verified to evaluate the seismic responses in the structure employing Plaxis 3D software. The effects of base flexibility (SSI) as well as increasing piles embedment depths on the seismic performance of high-rise structures are investigated.

.

Keywords: Soil-structure interaction; high-rise building seismic performance; direct approach; Plaxis 3D model.

1. INTRODUCTION

The need for increasing building height yet optimized design raises the importance for more accurate method of seismic performance assessment. The conventional non-interaction analysis of buildings without considering the influence of the subsurface is not always accurate or conservative. The interaction between the structure and subsurface lithology is necessary in order to design earthquake resistant structures and to evaluate the seismic safety of the building. The notable damages caused by the earthquakes that occurred in some cities, such as those in Mexico City 1985, Fukushima 2011, and Christchurch 2011, and other recent earthquakes, demonstrate the fact that local soil properties can play a significant role in determining seismic response of the structures under the earthquakes' motions. To solve soil-structure interaction problems, there are two main methods; the direct method [1-3] and the substructure method [4-6].

The Modelling of foundations and superstructures is generally found to be more straightforward and less complicated in comparison to the soil medium underneath [7]. Soil domain modelling techniques are Winkler foundation model, springs and dashpots model [8], discrete element cone model [9], beam on non-linear Winkler foundation model [10], contact interface model [11], and micro-element models. Beneficial effects of Soil-Structure Interaction (SSI) on structures could be; decrease in base shear, increase in damping ratio, and lengthening of natural period. However, detrimental consequences of SSI on structures can lead to site resonance, increase rocking of wall foundation, ground motion amplification, increase base shear of the frame bases, increase lateral displacements, and increase in story-drifts [12].

2. NUMERICAL APPROACH VERIFICATION

The verification of the three-dimensional numerical model is validated by comparing the results of numerical simulation and the results of experimental shaking table tests that have been attained by Zhang and Far [2]. The physical and mechanical properties in addition to the dimension of the numerical frame structure model and the ground soil as well as the scaled El-Centro earthquake

ground motion are the same as those selected in the experimental shaking table tests. Figure 1 shows the three-dimensional model of the scaled frame structure in Plaxis-3D software [13] and ETABS software [14] considering flexible-base and fixed-base, respectively.
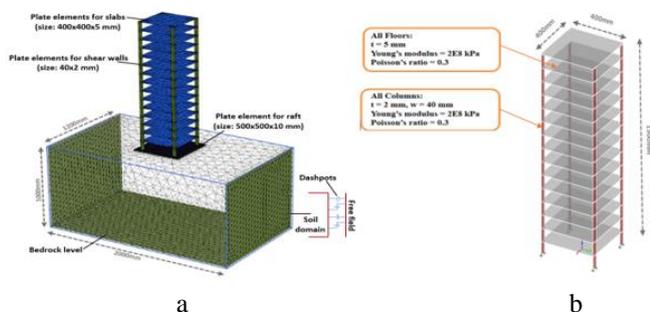

Fig 1. 3D numerical model of the scaled frame structure with; (a) flexible-base; (b) fixed-base

TABLE 1. Adopted strain compatible parameters and damping coefficients for the soil-frame structure system [2]

Earthquake Record	G/G_{max}	ξ (%)	Damping Coefficients
Scaled El-Centro	0.48	14.0	$\alpha = 5.245$ $\beta = 0.0028$

The observations attained from Fig. 2 indicate that both fixed-base and flexible-base numerical models have the enough accuracy to represent the structures seismic response under the influence of the earthquake record. Percentages of maximum lateral displacements errors in fixed-base and flexible-base cases are only 8.5% and 6.9%, respectively.
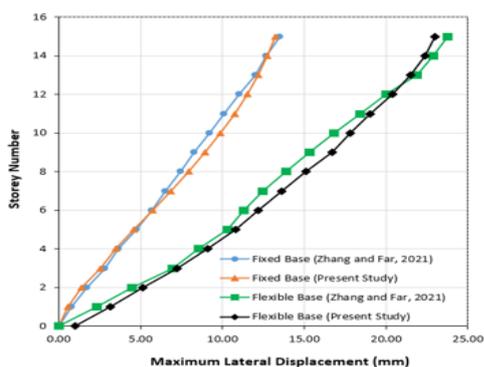

Fig2. Variations between numerical and experimental maximum lateral displacements of fixed-base and flexible-base models

3.MATERIALS AND METHODS

3.1Structural Description

25-story building structural analysis was performed by using ETABS software [14], which was confined to ECP 203-2020 [15], with the plan details illustrated in Fig. 3. The dynamic analysis was performed as per ECP 201-2012 [16] using the response spectrum analysis method.
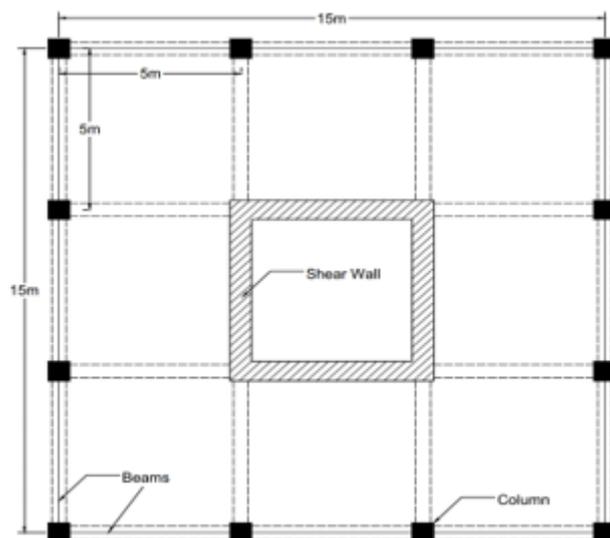

FIG 3. Detailed plan of the reference floor of the multi-story building in this study

The structural elements cross sections are preliminary designed according to the requirements of Egyptian code for design and construction of reinforced concrete structures, ECP 203-2020 [15]. All elements' sections are made from C35 concrete grade, with a compressive strength (f_{cu}) equal to 35 MPa. The Young's modulus of the concrete is $E_c = 4400$ $(f_{cu})^{0.5}$ (26,030 MPa), the reinforced concrete has a unit weight of 25 kN/m³, and a steel rebar made from B400DWR steel, with a yield strength (f_y) of 400 MPa. The reinforcement ratios of vertical concrete elements range from 1.3% to 2.8% with an average ratio of 2.1%. The increase in these ratios and amount of reinforcement results in larger overstrength factors [17]. In the dynamic analyses, cracked sections for the concrete elements are taken into consideration by multiplying gross section (I_g) of slabs, beams, columns, and shear walls by 0.25, 0.5, 0.7, and 0.35, respectively according to ECP 203-2020 [15]. The damping of 5%, which occurred within the structural members, is considered for the dynamic analysis. The fundamental frequency of the fixed-base building is found to be 0.449 Hz. From the results of the dynamic structural design, the building period is found to be 2.228s, and the effective mass ratios for the first three modes, and for the end of all modes, are found to be 0.8092 and 0.9383, respectively. The dimensions of the structural elements are summarized in Table 2 and indicated in Fig. 4.

TABLE 2. Summary of structural elements dimensions

Element Type	Story Level	Dimensions (m)
Column-C1	1 to 5	0.80 x 0.80
Column-C2	6 to 10	0.75 x 0.75
Column-C3	11 to 15	0.70 x 0.70
Column-C4	16 to 20	0.65 x 0.65
Coulmn-C5	21 to 25	0.60 x 0.60
Shear Walls	1 to 25	0.60m thick
Beams	1 to 25	0.30 x 0.80
Slabs	1 to 25	0.25m thick

The base reactions obtained from the structural analysis, which was conducted employing ETABS software [14], are utilized to design the foundation system using SAFE software [18]. The piled-raft foundation (substructure) system is safe against one-way shear and two-way (punching) shear criteria as per ECP 203-2020 [15]. The substructure design details are represented by the raft dimensions of length, width, and thickness are 22m, 22m, and 2m, respectively. This raft supported on 100 piles (10x10 piled configuration) with diameters equal to 0.6m. The piles have lengths (L) of 30m and spacings between piles of 2.278m as shown in Fig. 4.
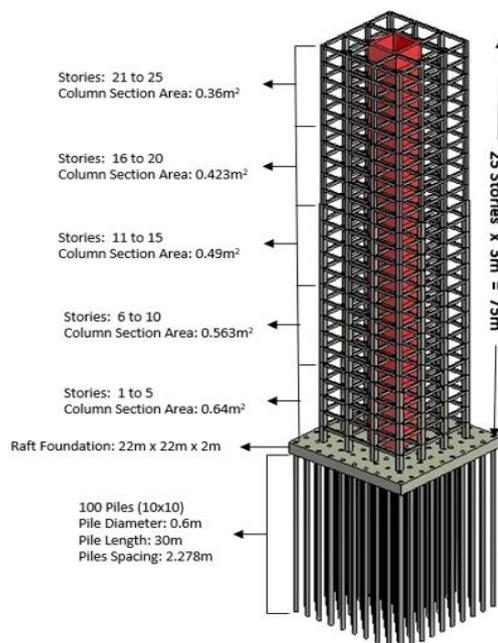

Fig 4. Designed structural sections of the 25-story building used in the analysis

3.2 **Geotechnical Characteristics and Earthquake Ground Motion**

The superstructure is founded on low compressible SILT - poorly graded SAND and the bedrock depth is 95m. This utilized geotechnical characteristics of the subsoil [3] are shown in Table 3. By employing ECP 202-2007 [19], the pile base resistance (F_{max}), axial skin resistance (F_{skin}), and bearing capacity (N_{pile}) in such φ-c soil are summarized in Table 4.

TABLE 3. Soil properties and parameters used in the study [3]

Parameter	Symbol	Magnitude	Unit
Unit Weight	γ	15.5	$(kN.m^{-3})$
Young's Modulus	E	28.0	$(MN.m^{-2})$
Poisson's Ratio	υ	0.33	-
Friction Angle	φ	22.0	(°)
Dilatancy Angle	ψ	1.0	(°)
Cohesion	c	24.0	$(kN.m^{-2})$
Void Ratio	e	0.882	-

TABLE 4. Base and axial skin pile resistances and pile bearing capacity in φ-c soil for different piles lengths

D (m)	L (m)	$F_{max.c}$ (kN)	$F_{skin.c}$ (kN)	$F_{max.φ}$ (kN)	$F_{skin.φ}$ (kN)	F_{max} (kN)	F_{skin} (kN)	N_{pile} (kN)
0.6	30	61	1305	2860	2328	2921	3633	6554
	36		1566		3327		4893	7814
	42		1827		7325		9152	12073
	48		2088		14751		16839	19760
	54		2349		25604		27953	30874

Where D and L are pile's diameter and length, $F_{max.c}$ and $F_{skin.c}$ are pile's base and axial skin resistances in c-soil, $F_{max.\varphi}$ and $F_{skin.\varphi}$ are pile's base and axial skin resistances in φ-soil.

Figures 5 and 6 elucidate the employed seismic input motions for the time-history dynamic analyses performed in this study, which are El-Centro and Hachinohe earthquakes records, that occurred in California, USA on May 18, 1940 and Tokachi-Oki, Japan on May 16, 1968, with magnitudes (M_w) of 6.9 and 7.2, times of 53.7s and 36s, and peak ground accelerations (PGA) of 0.349g and 0.229g, respectively, according to data obtained from the PEER Ground Motion Database [20].
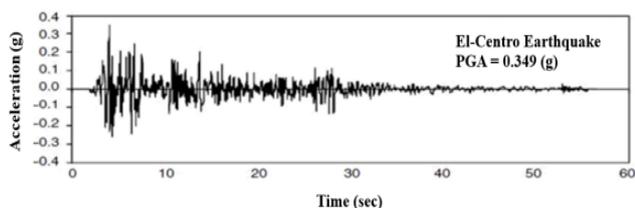
Fig 5. Utilized El-Centro earthquake acceleration record in the analysis [20]
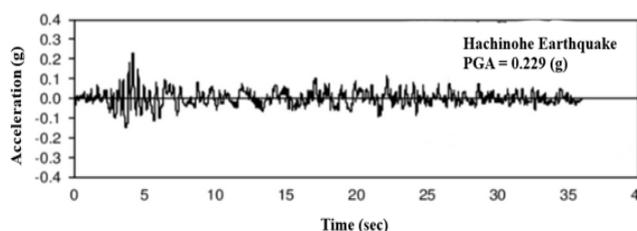
Fig 6. Utilized Hachinohe earthquake acceleration record in the analysis [20]

3.3 Modelling of Soil-Structure System with Finite Element Method

Using the direct approach requires employing a computer program that can simulate the behavior of both structure and soil with equal rigor simultaneously [21]. Plaxis 3D software package [13] was used to perform dynamic analyses for soil-structure interaction problems in which the Rayleigh coefficients, mass damping factors (α=0.758,0.284) and stiffness damping factors (β=0.012,0.024) considering El-Centro and Hachinohe earthquakes, respectively, were calculated taking into account the frequency-dependent damping that forms the different modes comprising the soil-foundation [2,3]. Soil elements, structural elements as shown in Fig. 4, interface elements, time-dependence loading indicated in Figs. 5 and 6, bedrock base, and lateral boundaries are the components of the soil-structure numerical model as illustrated in Fig. 7.
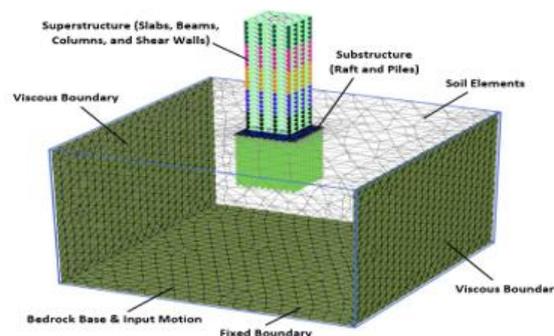

Fig 7. Components of the soil-structure system numerical model in Plaxis 3D

To represent the foundation-soil contact surface, interface elements were employed to allow for a proper modelling of SSI and provide the interactions between each pile, raft, and the surrounding soil. In Plaxis 3D, the pile was modelled as an embedded beam confined by the surrounding soil. The software considered the lateral and buckling behavior of the piles by default. In most of geotechnical simulations, the interfaces strength reduction factor (R_{inter}) of 0.75 was used to reduce the interface's shear strength [3]. Several researchers [2,3] have employed the adopted non-linear elastic-perfectly-plastic Mohr-Coulomb model to represent the dynamic SSI with aim of simulating the soil behavior under seismic loads. The free field boundary condition was set for the lateral boundaries of soil model that are simulated by absorbent boundaries and the compliant base boundary condition was set for the bottom boundary (bedrock base) of the soil model as indicated in Fig. 7. The distance between soil boundaries in the horizontal directions was equal to eight times raft's dimension and the depth of soil model determined according to the depth of bedrock indicated by the geotechnical characteristic of the soil (soil profile) as shown in Fig. 8.
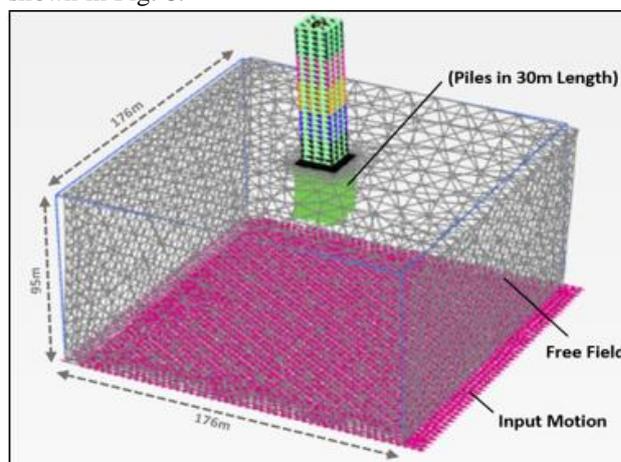

Fig 8. 25-story building with flexible-base model in Plaxis 3D

4.NUMERICAL INVESTIGATION AND PARAMETRIC STUDY

4.1Preface

In this research, non-linear dynamic analyses using time-history method and direct approach were performed to represent the dynamic SSI employing Plaxis 3D V21 [13]. These analyses were carried out for the 25-story building exposed to different earthquake loadings assuming fixed-base structure and flexible-base structure with piles lengths (L=30m). Additionally, different piles lengths more than 30m were proposed to investigate the increasing of piles embedment depths effects on the structure seismic response. Percentage of increasing embedment depths were 20%, 40%, 60%, and 80% resulting in piles lengths of 36m, 42m, 48m, and 54m, respectively as depicted in Fig. 9.
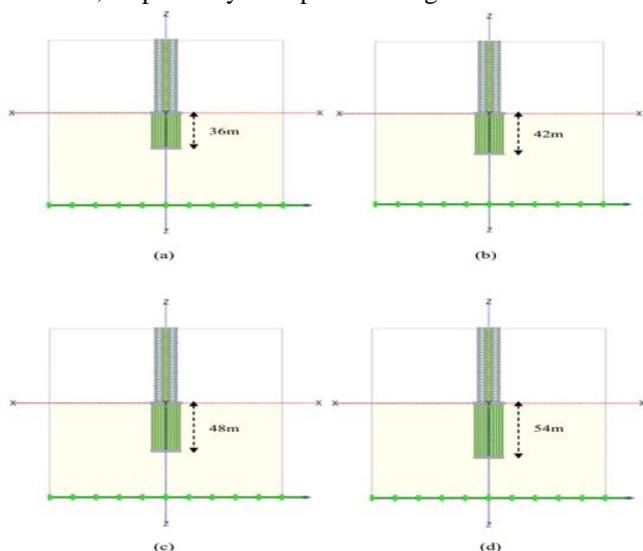
Fig 9. Flexible-base models in Plaxis 3D with piles lengths equal to; (a) 36m; (b) 42m; (c) 48m; (d) 54m

4.2Results and Discussions

4.2.1 Effects of SSI on the Structure Response

Converting building's fixed-base to a flexible-base, by simulating the soil, substructure elements, and superstructure elements in the same model, elucidates SSI effects on the building seismic performance. The flexible-base building model, attained employing Plaxis 3D, pointed out that the fundamental frequency and fundamental period equal to 0.4 Hz and 2.5s, respectively. The time history plots (accelerations and displacements), shown in Figs. 10 and 11, indicated that the building experienced greater acceleration and displacement for higher floor levels, with accelerations varying between 0.067g and 0.062g at the base floor, to 0.246g and 0.175g (70.5% and 76.4% of the applied earthquakes) on the top floor (story-25) of the building due to El-Centro and Hachinohe earthquakes, respectively.
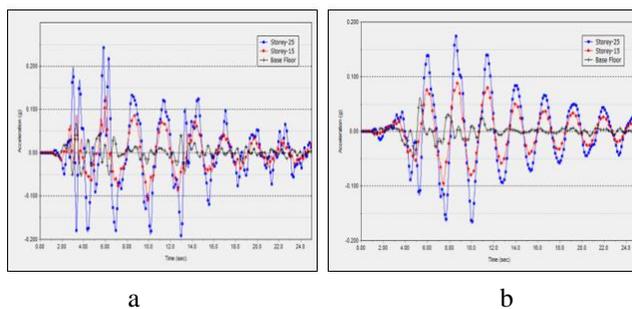

a   b

Fig 10. Time-acceleration plots of the different story levels in the building with 30m piles due to; (a) El-Centro earthquake; (b) Hachinohe earthquake
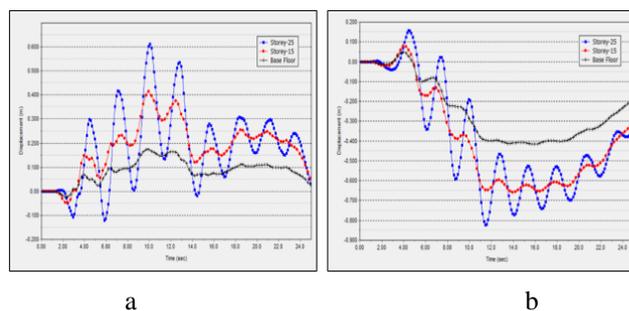

a   b

Fig 11. Time-displacement plots of the different story levels in the building with 30m piles due to; (a) El-Centro earthquake; (b) Hachinohe earthquake

Figures 12, 13, 14 show the maximum lateral displacements, inter-story drifts, and story shear forces of the structure under fixed-base and flexible-base conditions, respectively. As observed, the maximum displacements increased by 59.4% and 135.4% under the influence of SSI and applying El-Centro and Hachinohe earthquakes, respectively, the inter-story drifts of the structure considering SSI increased compared to rigid base case and presented an approximately vertical straight line, indicating that the inter-story drifts weren't alter much with higher stories, and the overall deflection curve is approximately linear. The story shear forces of the 25-story building decreased to some extent due to SSI. Additionally, the bases shears of the flexible-base structure were only 32.74% and 27.49% of that of fixed-base structure when subjected to El-Centro and Hachinohe earthquakes, respectively. It should be mentioned that not all shear forces of stories were reduced, as the shear forces of the 24th and 25th stories have been increased after taking the SSI into account, possible reason is the shear wall stiffness that considered same along building height in the numerical model.
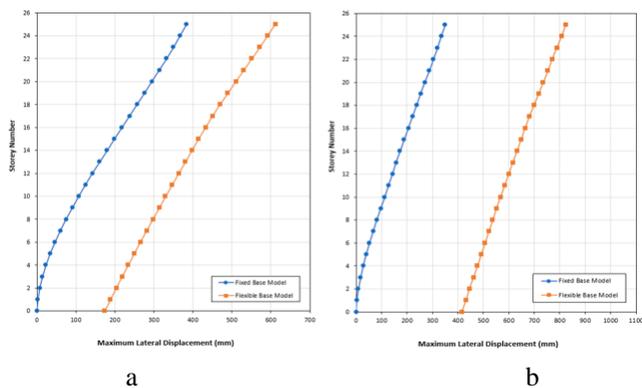
a   b

Fig 12. Variation in maximum lateral displacements considering fixed and flexible bases due to; (a) El-Centro earthquake; (b) Hachinohe earthquake
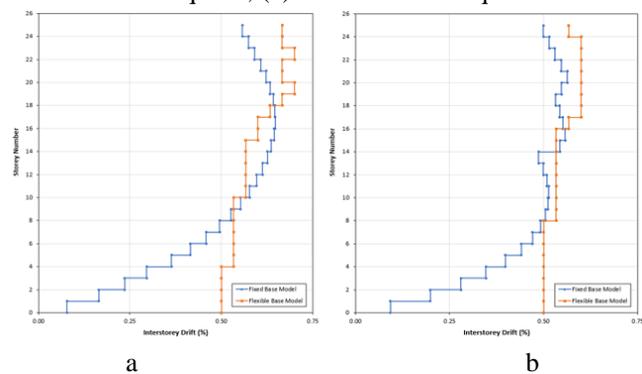

a   b

Fig 13. Variation in inter-story drifts considering fixed and flexible bases due to; (a) El-Centro earthquake; (b) Hachinohe earthquake
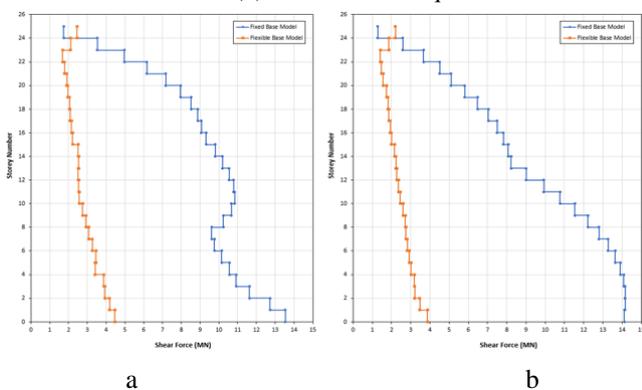

a   b

Fig 14. Variation in story shear forces considering fixed and flexible bases due to; (a) El-Centro earthquake; (b) Hachinohe earthquake

4.2.2 Effects of Increasing Embedment Depths of Piles on the Structure Response

Considering flexible-bases, Figs. from 15 to 18 show that increasing piles embedment depths by 20%, 40%, 60%, and 80%, reduces maximum accelerations through the building when subjected to El-Centro excitation by 15.0%, 21.5%, 22.4%, and 22.8%, respectively. Same response resulted under Hachinohe excitation as the maximum accelerations have been decreased by 12.6%, 13.7%, 14.3%, and 14.3%. These reductions occurred due to increasing of skin

resistance between foundations and soil strata, resulting in improving the response of building in accelerations and displacements resistance.
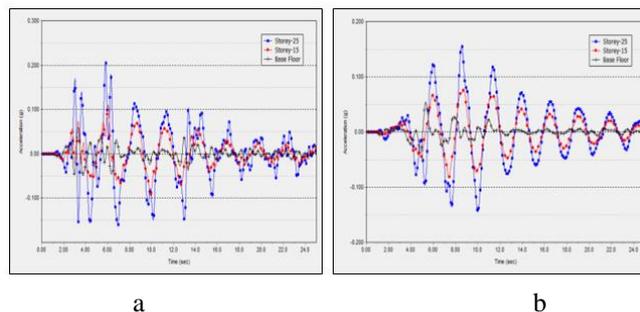

a   b

Fig 15. Time-acceleration plots of the different story levels in the building with 36m piles due to; (a) El-Centro earthquake; (b) Hachinohe earthquake
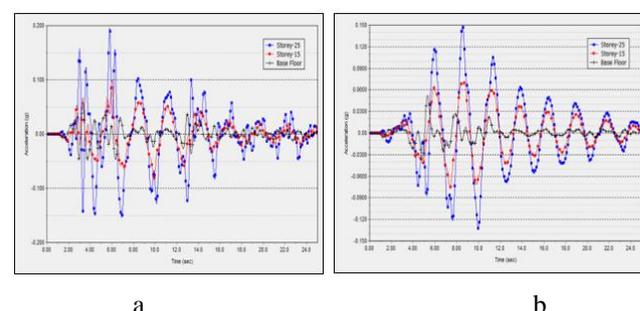

a   b

Fig 16. Time-acceleration plots of the different story levels in the building with 42m piles due to; (a) El-Centro earthquake; (b) Hachinohe earthquake
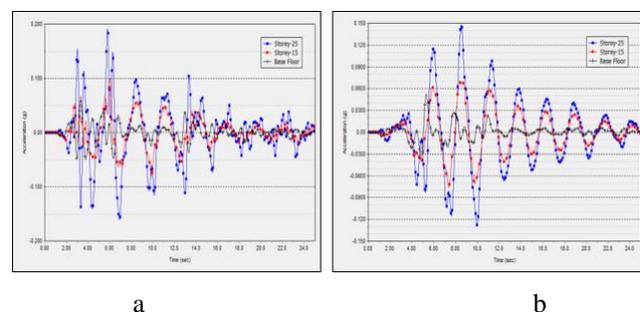

a   b

Fig 17. Time-acceleration plots of the different story levels in the building with 48m piles due to; (a) El-Centro earthquake; (b) Hachinohe earthquake
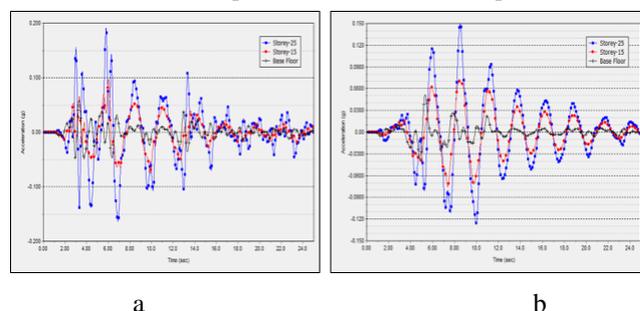

a   b

Fig 18. Time-acceleration plots of the different story levels in the building with 54m piles due to; (a) El-Centro earthquake; (b) Hachinohe earthquake

Figures from 19 to 22 depict that maximum displacements were reduced by 17.5%, 26.6%, 30.2%, and 32.2%, under influence of El-Centro earthquake, and 15.8%, 22.8%, 25.8%, and 26.7%, when subjected to Hachinohe earthquake, due to piles lengths of 36m, 42m, 48m, and 54m, respectively.
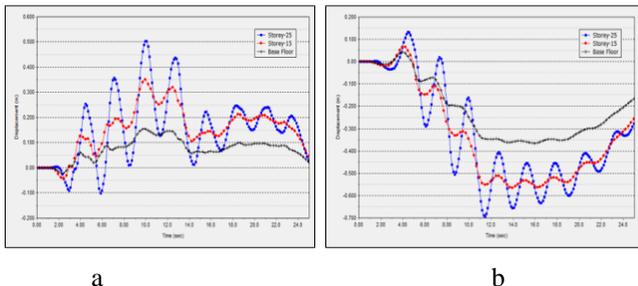

a   b

Fig 19. Time-displacement plots of the different story levels in the building with 36m piles due to; (a) El-Centro earthquake; (b) Hachinohe earthquake

a   b

Fig 20. Time-displacement plots of the different story levels in the building with 42m piles due to; (a) El-Centro earthquake; (b) Hachinohe earthquake

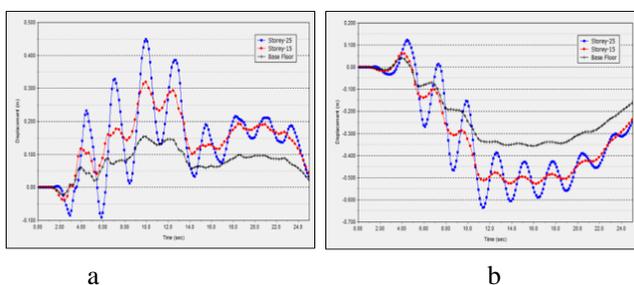a   b

Fig 21. Time-displacement plots of the different story levels in the building with 48m piles due to; (a) El-Centro earthquake; (b) Hachinohe earthquake

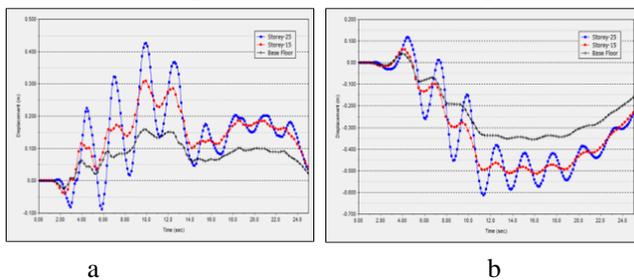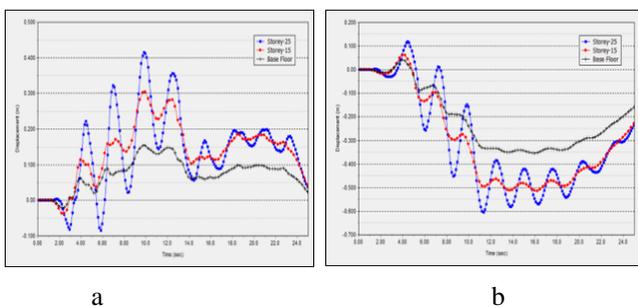a   b

Fig 22. Time-displacement plots of the different story levels in the building with 54m piles due to; (a) El-Centro earthquake; (b) Hachinohe earthquake

Variations in maximum lateral displacements, inter-story drifts, and story shear forces of the flexible-base building, with the mentioned piles lengths, indicated in Figs. 23, 24, and 25, respectively. The lateral displacements and inter-story drifts were decreased. However, using piles lengths more than 1.4L wasn't affecting significantly on the structure response, moreover, piles with 1.4L, 1.6L, and 1.8L lengths were found to provide approximately identical response. Consequently, considering the building seismic performance, 40% could be considered the optimum piles lengths increase for reducing the seismic response. It should be pointed out that increasing piles depths led to an increase in base shear and story shear forces. However, the base shear corresponding to building with piles lengths of 1.2L, 1.4L, 1.6L, and 1.8L were 36.93%, 38.66%, 38.96%, and 38.98%, in case of El-Centro excitation, and 30.71%, 32.18%, 33%, and 33.24%, in case of Hachinohe excitation, of that of fixed-base building, respectively.
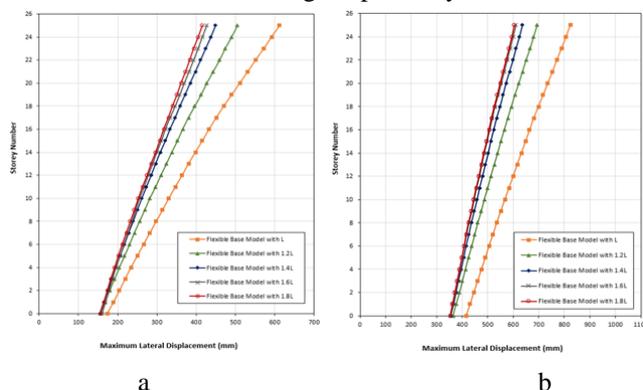

a   b

Fig 23. Variation in maximum lateral displacements with different piles lengths due to; (a) El-Centro earthquake; (b) Hachinohe earthquake
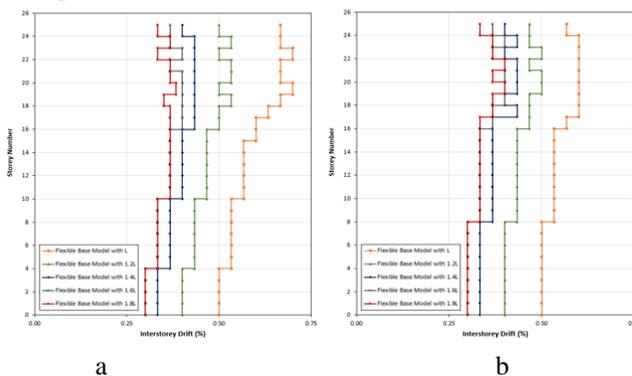

a   b

Fig 24. Variation in inter-story drifts with different piles lengths due to; (a) El-Centro earthquake; (b) Hachinohe earthquake
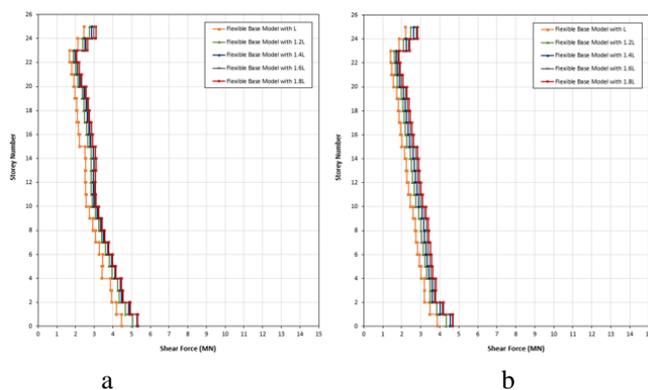
a   b

Fig 25. Variation in story shear forces with different piles lengths due to; (a) El-Centro earthquake; (b) Hachinohe earthquake

5.CONCLUSION

Considering SSI for a building supported by piled-raft, lengthens the building fundamental period by 12.2%, and results in increased maximum lateral displacements and inter-story drifts as well as reduced base shear. The story shear forces of the building have been decreased to some extent after taking the SSI into account, except for 24th and 25th stories, possible reason is the shear wall stiffness that considered same along building height in the numerical model.

Under the influence of El-Centro seismic excitation, increasing piles embedment depths by 20% up to 80%, leads to reduction in maximum accelerations of the building ranging from 15% to 22.8% corresponding to reduction in maximum displacements by 17.5% to 32.2%. Same response resulted under Hachinohe seismic motion as the maximum accelerations have been decreased by 12.6% to 14.3%, and maximum displacements decreased by 15.8% to 26.7%.

The results of inter-story drifts also show a decrease, representing more stiffer building seismic performance. It is worth mentioning that the base shear and story shear forces increase by increasing of piles embedment depths. Nevertheless, maximum shear of bases, using 1.8L, are only 38.98% and 33.24% of that of fixed-base structure when subjected to El-Centro and Hachinohe earthquakes, respectively.

It's obvious that piles with 1.4L, 1.6L, and 1.8L lengths are providing approximately identical response. Consequently, increasing embedment depth more than 40% doesn't affect significantly on the structure response. Therefore, 40% could be considered as an optimum piles' lengths increase for improving the building seismic performance. This ratio depends mainly on the building height and the subsurface lithology conditions.

REFERENCES

[1]. Tabatabaiefar, H.R. and Massumi, A. (2010). "A simplified method to determine seismic responses of reinforced concrete moment resisting building frames under influence of soil structure interaction." Soil Dynamics and Earthquake Engineering, 30(11), pp.1259-1267.

[2]. Zhang, X., and Far, H. (2021). "Effects of dynamic soil-structure interaction on seismic behavior of high-rise buildings." Bull. Earthq. Eng. 20, 3443–3467. doi:10.1007/s10518-021-01176-z.

[3]. Bariker, P.; Kolathayar, S. (2022). "Dynamic Soil Structure Interaction of a High-Rise Building Resting over a Finned Pile Mat." Infrastructures 2022, 7, 142. https://doi.org/10.3390/infrastructures7100142.

[4]. Hassani, N., Bararnia, M., and Ghodrati Amiri, G. (2018). Effect of soil-structure interaction on inelastic displacement ratios of degrading structures. Soil Dyn. Earthq. Eng. 104, 75–87. doi:10.1016/j. soildyn.2017.10.004.

[5]. Mercado, J. A., Arboleda-Monsalve, L. G., Mackie, K., and Terzic, V. (2020). "Evaluation of substructure and direct modeling approaches in the seismic response of tall buildings." Geo-Congress 2020, 30–40. doi:10.1061/9780784482810.004.

[6]. Oz, I., Senel, S. M., Palanci, M., and Kalkan, A. (2020). "Effect of soil structure interaction on the seismic response of existing low and mid-rise RC buildings." Appl. Sci. 10, 8357(1–21). doi:10.3390/app10238357.

[7]. Bhattacharya, K., and Dutta, S. C. (2004). "Assessing lateral period of building frames incorporating soil-flexibility." J. Sound Vib. 269, 795–821. doi:10.1016/S0022-460X (03) 00136-6.

[8]. Gazetas, G. (1991). "Formulas and charts for impedances of surface and embedded foundations." J. Geotechnical Eng. 117 (9), 1363–1381. doi:10.1061/(asce)0733-9410(1991) 117:9(1363).

[9]. Wolf, J. (1994). "Foundation vibration analysis using simple physical models." Upper Saddle River, NJ: Prentice Hall Co.: Pearson Education).

[10]. Raychowdhury, P. (2008). Nonlinear Winkler-based shallow foundation model for performance assessment of seismically loaded structures. Ph.D. thesis, PhD thesis. San Diego: University of California.

[11]. Gajan, S., and Kutter, B. L. (2009). "Contact interface model for shallow foundations subjected to combined cyclic loading." J. Geotechnical Geo-environmental Eng. 135, 407–419. doi:10.1061/(asce)1090 0241 (2009)135:3 (407).

[12]. Wolf, J.P. and Deeks, AJ. (2004). "Foundation Vibration Analysis." A Strength-of Materials Approach, Elsevier, Oxford, UK.

[13]. Brinkgreve RB. Plaxis 3D Software. Netherland: Bentley; 2020.

[14]. ETABS Software, "Integrated Building Design Software," Computers and Structures Inc.

[15]. ECP-203 (2020). "Egyptian code for Design and Construction of Reinforced Concrete Structures." National Center for Researches of Housing and Construction, Ministry of Housing, Ministerial Decree No. 612.

[16]. ECP-201 (2012). "Egyptian code for Calculation of Loads and Forces in Structural Works and Buildings." National Center for Researches of Housing and Construction, Ministry of Housing, Ministerial Decree No. 431.

[17]. Trejo, D., Link, B. T., and Barbosa, R. A. (2016). "Effect of Reinforcement Grade and Ratio on Seismic Performance of Reinforced Concrete Columns." ACI Structural Journal, V. 113, No. 5, September-October 2016. MS No. S-2014-217.R2, doi: 10.14359/51689015.

[18]. SAFE Software, "Design of Slabs, Mats and Footings Software," Computers and Structures Inc.

[19]. ECP-202 (2007). "Egyptian code for Soil Mechanics and Foundation Design and Construction." National Center for Researches of Housing and Construction, Ministry of Housing, Ministerial Decree No. 139.

[20]. Peer Ground Motion Database. Available online: https://ngawest2.berkeley.edu

[21]. Kramer, S. (1996). Geotechnical earthquake engineering. Upper Saddle River, NJ): Prentice Hall.